Journal of Applied Analysis and Computation
Volume *, Number *, * *, 1–21
Website:http://jaac-online.com/
DOI:10.11948/*.1

BIFURCATION ANALYSIS AND CHAOS OF A MODIFIED HOLLING−TANNER MODEL WITH DISCRETE TIME

Qingkai Xu and Chunrui Zhang†

Abstract In this paper, we consider a classical Holling-Tanner model with discrete time. The dynamical behavior of the model is given by using both theoretical analysis and numerical simulation. We use the central manifold theorem and bifurcation theory to demonstrate that the system will undergo Hopf bifurcation and Flip bifurcation at the positive equilibrium point. By using Lyapunov exponent, we show that the system can undergo the path from stability to Flip(Hopf) bifurcation to chaos, and then we verify the correctness of the theoretical results via numerical simulations.

Keywords Holling-Tanner model, Flip bifurcation, Hopf bifurcation, Chaos

MSC(2010) 34C23, 37N25.

1. Introduction

The predator-prey model is a classical two-species biomathematical model and has been extensively studied [1–5]. A typical class of predator-prey system is called the Leslie model [6–8], and its general form is as follows (Mathsen and Freedman [9,10], Huang and Hsu [11])

$$\begin{cases} \frac{dx}{dt} = rx(1-\frac{x}{K}) - p(x)y, \\ \frac{dy}{dt} = sy(1-\frac{y}{hx}), \end{cases} \tag{1.1}$$

where $x(t)$ and $y(t)$ represent the population densities of prey and predators with respect to time t, and r and s describe the intrinsic growth ratio of prey and predators, respectively. Moreover, K and h describe the carrying ability and the food quantity index of the prey. The functional response [12, 13] of predators to prey density is represented by $p(x)$. The term $\frac{y}{hx}$ is called Leslie-Gower [14, 15] term.

Some common types of functional responses include Holling I-IV functional response [16–19], Crowley-Martin functional response [20], ratio dependent functional response [21] and so on. When $p(x)$ is selected as the commonly applied Holling Type II functional response $\frac{mx}{n+x}$, then the system (1.1) becomes as the Holling-

†the corresponding author. Email address:math@nefu.edu.cn(Chunrui Zhang)
[1]Department of Mathematics, Northeast Forestry University, Harbin 150040, China

Tanner system [22–24]:

$$\begin{cases} \frac{dx}{dt} = rx(1-\frac{x}{K}) - \frac{mxy}{n+x}, \\ \frac{dy}{dt} = sy(1-\frac{y}{hx}), \end{cases} \tag{1.2}$$

where m represents the maximum predation ratio and n is regarded as the semi-saturation constant.

In models (1.1) and (1.2), predators have only a single food source to survive, and when their particular prey is scarce, predators also become endangered. While in nature, there are some special predators, in addition to hunting specific prey, can also feed on other species as a food source, such predators are called generalist predators. Based on the Holling-Tanner model (1.2), Daher Okiye and Aziz-Alaoui [25, 26] proposed the improved Holling-Tanner model:

$$\begin{cases} \frac{dx}{dt} = rx(1-\frac{x}{K}) - \frac{mxy}{n+x}, \\ \frac{dy}{dt} = sy(1-\frac{y}{hx+K_2}), \end{cases} \tag{1.3}$$

where $K_2 > 0$ is the additional constant carrying capacity acquired by predators from all other sources of food.

To simplify parameters, define $x = K\bar{x}$, $y = hK\bar{y}$, $t = \frac{\tau}{r}$, drop the bar and still remember t as the time scale, then system (1.3) becomes

$$\begin{cases} \frac{dx}{dt} = x(1-x) - \frac{axy}{x+k_1}, \\ \frac{dy}{dt} = cy(1-\frac{y}{x+k_2}), \end{cases} \tag{1.4}$$

where $a = \frac{mh}{r}$, $c = \frac{s}{r}$, $k_1 = \frac{n}{K}$, $k_2 = \frac{K_2}{hK}$, and all of them are positive.

The system (1.3) and (1.4) has been widely used and studied. For example, Li and Song [27] used the Dulac criterion and Liapunov function to conduct a detailed analysis of the global stability of a unique positive equilibrium point. Aziz-Alaoui and Daher Okiye [25] provided several sufficient conditions to guarantee the global stability of the unique positive trivial equilibrium point. However, most of these studies are based on continuous models, and discrete models are rarely discussed at present. Besides, many studies have shown that when the intergenerational relationship of populations is non-overlapping, constructing discrete models by difference equation will more closely align with the objective reality [28]. In addition, compared with the continuous system, the discrete model has more complex dynamical behavior [29, 30], so it has more practical guiding value for us. In this paper, model (1.4) is discretized by explicit Euler method [31], and then the dynamical properties of the improved Holling-Tanner system will be discussed.

After discretizing model (1.4) by explicit Euler method, we can get the following discrete modified Holling-Tanner model:

$$\begin{cases} x_{n+1} = x_n + \tau[x_n(1-x_n) - \frac{ax_ny_n}{x_n+k_1}], \\ y_{n+1} = y_n + \tau[cy_n(1-\frac{y_n}{x_n+k_2})], \end{cases} \tag{1.5}$$

where $\tau > 0$ refers to the step length of (1.5).

This article is organized as follows. In section 2, we study the existence and stability of boundary equilibrium points and positive equilibrium points of system

(1.5) respectively. Then we discuss Flip bifurcation and Hopf bifurcation around the unique positive equilibrium point when the bifurcation parameter τ fluctuates within a small region of specific curves in Section 3. In section 4, chaos scenarios are discussed by numerical simulation, and the maximum Lyapunov exponent and phase diagrams are provided to illustrate our theoretical results.

2. The existence and stability of equilibrium points

Here, the equilibrium points of model (1.5) and their types will be discussed. By solving the following equation

$$\begin{cases} x = x + \tau[x(1-x) - \frac{axy}{x+k_1}], \\ y = y + \tau[cy(1 - \frac{y}{x+k_2})], \end{cases} \tag{2.1}$$

and through simple calculations, we can acquire the following Lemma 2.1.

Lemma 2.1.

(i) The system (1.5) *has a trivial equilibrium* $E_1 = (0, 0)$ *and two boundary equilibria* $E_2 = (1, 0)$, $E_3 = (0, k_2)$*;*

(ii) The positive equilibrium of system (1.5) *must satisfy the following expression*

$$x^2 - (1 - a - k_1)x + ak_2 - k_1 = 0,$$

which can be seen as a quadratic equation with x *as the root in the interval* $(0, 1)$*.*

2.1. Boundary equilibria and their types

The Jacobi matrix of the linear equation of (1.5) at any equilibrium point $E(x, y)$ takes the following form:

$$J(x,y) = \begin{pmatrix} 1 + \tau(1 - 2x - \frac{ak_1y}{(x+k_1)^2}) & -\frac{a\tau x}{x+k_1} \\ \frac{c\tau y^2}{(x+k_2)^2} & 1 + c\tau - \frac{2c\tau y}{x+k_2} \end{pmatrix}. \tag{2.2}$$

Suppose that the characteristic equation of the Jacobian matrix has two roots, λ_1 and λ_2. By calculating the eigenvalues corresponding to each equilibrium point, we can easily obtain the following theorems.

Theorem 2.1. *For the trivial equilibrium* E_1*, the eigenvalues get* $\lambda_1 = 1 + \tau$, $\lambda_2 = 1 + c\tau$*. So* E_1 *is a source with eigenvalues* $|\lambda_1| > 1$, $|\lambda_2| > 1$*, and it is locally unstable.*

Theorem 2.2. *For the boundary equilibrium* E_2*, the eigenvalues get* $\lambda_1 = 1 - \tau$, $\lambda_2 = 1 + c\tau$*, where* $0 < \tau < 2$*. So* E_2 *is a saddle with eigenvalues* $|\lambda_1| < 1$, $|\lambda_2| > 1$*.*

Theorem 2.3. *For the boundary equilibrium* E_3*, with the eigenvalues* $\lambda_1 = 1 + \tau - \frac{a\tau k_2}{k_1}$, $\lambda_2 = 1 - c\tau$*.*

(A_1) E_3 *is a sink point, if* $0 < \tau < \min(\frac{2}{c}, \frac{-2k_1}{k_1 - ak_2})$*, and* $k_2 > \frac{k_1}{a}$*, with eigenvalues* $|\lambda_1| < 1$, $|\lambda_2| < 1$*, and* E_3 *is locally asymptotically stable;*

(A_2) *E_3 is a source point, if* $k_2 < \frac{k_1}{a}$ *and* $\tau > \frac{2}{c}$, *or* $k_2 > \frac{k_1}{a}$ *and* $\tau > \max(\frac{2}{c}, \frac{-2k_1}{k_1-ak_2})$, *with eigenvalues* $|\lambda_1| > 1$, $|\lambda_2| > 1$, *and E_3 is locally unstable;*

(A_3) *E_3 is a saddle point, if* $\frac{2}{c} < \tau < \frac{-2k_1}{k_1-ak_2}$ *and* $k_1 - ak_2 < 0$, *with eigenvalues* $|\lambda_1| < 1$ *and* $|\lambda_2| > 1$; *or* $k_2 < \frac{k_1}{a}$ *and* $0 < \tau < \frac{2}{c}$, *or* $\frac{-2k_1}{k_1-ak_2} < \tau < \frac{2}{c}$ *and* $k_2 > \frac{k_1}{a}$ *, with eigenvalues* $|\lambda_1| > 1$ *and* $|\lambda_2| < 1$;

(A_4) *Flip bifurcation occurs at E_3 if* $\begin{cases} 0 < \tau < \frac{-2k_1}{k_1-ak_2} \\ \tau = \frac{2}{c} \\ k_1 - ak_2 < 0 \end{cases}$, *with eigenvalues* $\lambda_2 = -1$ *and* $|\lambda_1| < 1$, *or* $\tau = \frac{-2k_1}{k_1-ak_2} < \frac{2}{c}$ *with eigenvalues* $\lambda_1 = -1$ *and* $|\lambda_2| < 1$;

(A_5) *Transcritical bifurcation occurs at E_3 if* $\begin{cases} k_1 - ak_2 = 0 \\ \tau < \frac{2}{c} \end{cases}$, *with eigenvalves* $\lambda_1 = 1$ *and* $|\lambda_2| < 1$.

2.2. Positive equilibria and their types

According to Lemma 2.1, the positive equilibrium $E(x, y)$ of model (1.5) must satisfy the equation in (ii).Therefore, according to the range of values with different parameters, the existence of the positive equilibrium point has different situations.

2.2.1. The existence analysis of the positive equilibrium point

By several calculations, we can acquire the following conclusions.

Lemma 2.2. *The positive equilibrium point of model* (1.5) *has the following situations:*

(i) The model (1.5) *has no positive equilibrium if* $\begin{cases} k_2 > \frac{(1-a-k_1)^2+4k_1}{4a} \\ k_1 < 1-a, a < 1 \end{cases}$ *,or* $\begin{cases} k_2 \geq \frac{k_1}{a} \\ k_1 \geq 1-a \end{cases}$;

(ii) The model (1.5) *has a unique positive equilibrium*
$E_{*1}(\frac{1-a-k_1+\sqrt{(1-a-k_1)^2-4(ak_2-k_1)}}{2}, \frac{1-a-k_1+\sqrt{(1-a-k_1)^2-4(ak_2-k_1)}}{2} + k_2)$ *if* $k_2 < \frac{k_1}{a}$,
or $E_{*2}(1-a-k_1, 1-a-k_1+k_2)$ *if* $\begin{cases} k_2 = \frac{k_1}{a} \\ k_1 < 1-a, a < 1 \end{cases}$;

(iii) The model (1.5) *has positive equilibrium* $E_{*3}(\frac{1-a-k_1}{2}, \frac{1-a-k_1}{2} + k_2)$ *with multiplicity 2 if* $\begin{cases} k_2 = \frac{(1-a-k_1)^2+4k_1}{4a} \\ k_1 < 1-a, a < 1 \end{cases}$;

(iv) The model (1.5) *has two positive equilibria*
$E_{*4}(\frac{1-a-k_1+\sqrt{(1-a-k_1)^2-4(ak_2-k_1)}}{2}, \frac{1-a-k_1+\sqrt{(1-a-k_1)^2-4(ak_2-k_1)}}{2} + k_2)$ *and*
$E_{*5}(\frac{1-a-k_1-\sqrt{(1-a-k_1)^2-4(ak_2-k_1)}}{2}, \frac{1-a-k_1-\sqrt{(1-a-k_1)^2-4(ak_2-k_1)}}{2} + k_2)$
if $\begin{cases} \frac{k_1}{a} < k_2 < \frac{(1-a-k_1)^2+4k_1}{4a} \\ k_1 < 1-a, a < 1 \end{cases}$.

Remark 2.1. In biology, we are more concerned with the dynamic properties at the unique positive equilibrium point, so the condition of (ii) in Lemma 2.2 will be satisfied in our future discussions. And furthermore, the equilibrium point E_{*1} is chosen without loss of generality.

To facilitate calculation, denote $\alpha = 1-a-k_1, \beta = \sqrt{(1-a-k_1)^2 - 4(ak_2-k_1)}$, then the unique positive equilibrium $E_*(x^*, y^*)$ of system (1.5) can be written in the following form:
$E_*(x^*, y^*) = (\frac{\alpha+\beta}{2}, \frac{\alpha+\beta}{2}+k_2) = (\frac{1-a-k_1+\sqrt{(1-a-k_1)^2-4(ak_2-k_1)}}{2}, \frac{1-a-k_1+\sqrt{(1-a-k_1)^2-4(ak_2-k_1)}}{2} + k_2)$.

2.2.2. The stability analysis of the unique positive equilibrium $E_*(x^*, y^*)$

The value of the Jacobian $J(x, y)$ around unique point $E_*(\frac{\alpha+\beta}{2}, \frac{\alpha+\beta}{2} + k_2)$ is

$$J(E_*) = \begin{pmatrix} 1+\tau[1-(\alpha+\beta)-\frac{2ak_1(\alpha+\beta+2k_2)}{(\alpha+\beta+2k_1)^2}] & -\frac{a\tau(\alpha+\beta)}{\alpha+\beta+2k_1} \\ c\tau & 1-c\tau \end{pmatrix}, \tag{2.3}$$

then the characteristic equation related to $J(E_*)$ is

$$f(\lambda) = \lambda^2 - l_1\lambda + l_2, \tag{2.4}$$

where
$l_1 = tr(J) = 2+\tau[1-c-(\alpha+\beta)-\frac{2ak_1(\alpha+\beta+2k_2)}{(\alpha+\beta+2k_1)^2}]$,
$l_2 = \det(J) = 1+\tau[1-c-(\alpha+\beta)-\frac{2ak_1(\alpha+\beta+2k_2)}{(\alpha+\beta+2k_1)^2}]+c\tau^2[-1+\alpha+\beta+\frac{2ak_1(\alpha+\beta+2k_2)}{(\alpha+\beta+2k_1)^2}+\frac{a(\alpha+\beta)}{\alpha+\beta+2k_1}]$.
And we have

$$f(1) = 1-l_1+l_2, \quad f(-1) = 1+l_1+l_2.$$

Lemma 2.3. *[32, 33] Suppose that $\phi(\lambda) = \lambda^2 + P\lambda + Q$, and $\phi(1) > 0$ with $\lambda, \tilde{\lambda}$ are roots of $\phi(\lambda) = 0$. Then the following conclusions hold:*

(A_1) *$|\lambda| < 1$ and $\left|\tilde{\lambda}\right| < 1$ if and only if $\phi(-1) > 0$ and $Q < 1$;*

(A_2) *$|\lambda| < 1$ and $\left|\tilde{\lambda}\right| > 1$ if and only if $\phi(-1) < 0$;*

(A_3) *$|\lambda| > 1$ and $\left|\tilde{\lambda}\right| > 1$ if and only if $\phi(-1) > 0$ and $Q > 1$;*

(A_4) *λ and $\tilde{\lambda}$ are a pair of conjugate complex roots and $|\lambda| = \left|\tilde{\lambda}\right| = 1$ if and only if $-2 < P < 2$ and $Q = 1$.*

The following Theorem 2.4 behaves the local dynamical properties of the unique positive point $E_*(x^*, y^*)$ from Lemma 2.3.

Theorem 2.4. *Assume that λ_1 and λ_2 are the eigenvalues of $f(\lambda)$. Then the following propositions at $E_*(x^*, y^*)$ hold:*

(A_1) *$E_*(x^*, y^*)$ is a sink point if and only if $l_1 < |1+l_2|$, and $l_2 < 1$, so $E_*(x^*, y^*)$ is locally asymptotically stable;*

(A_2) *$E_*(x^*, y^*)$ is a source point if and only if $l_1 < |1 + l_2|$, and $l_2 > 1$, so $E_*(x^*, y^*)$ is locally unstable;*

(A_3) *$E_*(x^*, y^*)$ is a saddle if and only if $l_1 < \min\{1 + l_2, -(1 + l_2)\}$;*

(A_4) *Flip bifurcation occurs at $E_*(x^*, y^*)$ if and only if $l_1 = -(1 + l_2)$ and $|l_2| < 1$;*

(A_5) *Hopf bifurcation occurs at $E_*(x^*, y^*)$ if and only if $-2 < l_1 < 2$, and $l_2 = 1$.*

Proof. According to Lemma 2.3, (A_1), (A_2) and (A_3) can be obtained easily.

For (A_4), Flip bifurcation occurs at $E_*(x^*, y^*)$ if and only if $\begin{cases} {l_1}^2 - 4l_2 > 0 \\ f(-1) = 0 \\ |\lambda_2| < 1 \end{cases}$, then we can obtain $l_1 = -(1 + l_2)$ and $|l_2| < 1$; For (A_5), Hopf bifurcation occurs at $E_*(x^*, y^*)$ if and only if $\begin{cases} f(1) > 0 \\ l_2 = 1 \\ -2 < l_1 < 2 \end{cases}$, then we can obtain $-2 < l_1 < 2$, and $l_2 = 1$. □

3. Bifurcation analysis at $E_*(x^*, y^*)$

In this section, the existence conditions and associated results of Flip bifurcation and Hopf bifurcation of the model (1.5) around the unique equilibrium point E_* will be obtained by the central manifold theorem and bifurcation theorem [34, 37].

3.1. Flip bifurcation at E_*

First, we point out how model (1.5) undergoes Flip bifurcation around its unique positive $E_*(\frac{\alpha+\beta}{2}, \frac{\alpha+\beta}{2} + k_2)$ when τ is selected as the bifurcation parameter. The necessary condition for Flip bifurcation to occur is determined by the following curve:

$$U_1 = \left\{ (a, c, k_1, k_2, \tau) \in R_+^5 : \tau = \tau^* = \frac{d_2 + \sqrt{d_2^2 - 16d_1}}{2d_1}, |l_2| < 1, k_2 < \frac{k_1}{a} \right\},$$

where $l_2 = det(J) = 1 + \tau[1 - c - (\alpha + \beta) - \frac{2ak_1(\alpha+\beta+2k_2)}{(\alpha+\beta+2k_1)^2}] + c\tau^2[-1 + \alpha + \beta + \frac{2ak_1(\alpha+\beta+2k_2)}{(\alpha+\beta+2k_1)^2} + \frac{a(\alpha+\beta)}{\alpha+\beta+2k_1}]$ and $d_1 = c[-1 + \alpha + \beta + \frac{2ak_1(\alpha+\beta+2k_2)}{(\alpha+\beta+2k_1)^2} + \frac{a(\alpha+\beta)}{\alpha+\beta+2k_1}]$, $d_2 = -2[1 - c - (\alpha + \beta) - \frac{2ak_1(\alpha+\beta+2k_2)}{(\alpha+\beta+2k_1)^2}]$.

3.1.1. Existence condition of Flip bifurcation at E_*

The Jacobian matrix $J(x, y)$ evaluated at the unique positive equilibrium $E_*(x^*, y^*)$ is the same as that of (2.3).

Let $X_n = x_n - x^*, Y_n = y_n - y^*$, which transforms the positive equilibrium $E_*(x^*, y^*)$ to point $(0, 0)$ and model (1.5) to

$$\begin{cases} X_{n+1} = X_n + \tau[(X_n + x^*)(1 - X_n - x^*) - \frac{a(X_n+x^*)(Y_n+y^*)}{X_n+x^*+k_1}], \\ Y_{n+1} = Y_n + \tau[c(Y_n + y^*)(1 - \frac{Y_n+y^*}{X_n+x^*+k_2})], \end{cases} \tag{3.1}$$

Using Taylor expansion at the point $E_*(x^*, y^*)$ yields the following expression:

$$\begin{pmatrix} X_{n+1} \\ Y_{n+1} \end{pmatrix} = J|_{(x^*,y^*)} \begin{pmatrix} X_n \\ Y_n \end{pmatrix} + \tau \begin{pmatrix} \varphi(X_n, Y_n) \\ \psi(X_n, Y_n) \end{pmatrix}, \tag{3.2}$$

where
$\varphi(X_n, Y_n) = A_{13}X_n^2 + A_{14}X_nY_n + A_{15}Y_n^2 + A_{16}X_n^3 + A_{17}X_n^2Y_n + A_{18}X_nY_n^2 + A_{19}Y_n^3 + O((|X_n| + |Y_n|)^4)$,
$\psi(X_n, Y_n) = A_{23}X_n^2 + A_{24}X_nY_n + A_{25}Y_n^2 + A_{26}X_n^3 + A_{27}X_n^2Y_n + A_{28}X_nY_n^2 + A_{29}Y_n^3 + O((|X_n| + |Y_n|)^4)$,
$A_{13} = -1 + \frac{ak_1y^*}{(x^*+k_1)^3}, A_{14} = -\frac{ak_1}{(x^*+k_1)^2}, A_{15} = 0, A_{16} = -\frac{ak_1y^*}{(x^*+k_1)^4}, A_{17} = \frac{ak_1}{(x^*+k_1)^3}$,
$A_{18} = 0, A_{19} = 0, A_{23} = -\frac{cy^{*2}}{(x^*+k_2)^3}, A_{24} = \frac{2cy^*}{(x^*+k_2)^2}, A_{25} = -\frac{c}{(x^*+k_2)}, A_{26} = \frac{cy^{*2}}{(x^*+k_2)^4}, A_{27} = \frac{-2cy^*}{(x^*+k_2)^3}, A_{28} = \frac{c}{(x^*+k_2)^2}, A_{29} = 0.$
We give parameter τ a small perturbation δ, i.e.,$\tau = \tau^* + \delta, |\delta| \ll 1$, and the system (3.2) becomes

$$\begin{pmatrix} X_{n+1} \\ Y_{n+1} \end{pmatrix} = \begin{pmatrix} 1 + (\tau^* + \delta)[1 - 2x^* - \frac{ak_1y^*}{(x^*+k_1)^2}] & -\frac{a(\tau^*+\delta)x^*}{x^*+k_1} \\ c(\tau^* + \delta) & 1 - c(\tau^* + \delta) \end{pmatrix} \begin{pmatrix} X_n \\ Y_n \end{pmatrix} + (\tau^* + \delta) \begin{pmatrix} \varphi(X_n, Y_n) \\ \psi(X_n, Y_n) \end{pmatrix}, \tag{3.3}$$

The characteristic polynomial of (3.3) is expressed by

$$g(\lambda) = \lambda^2 - p_1\lambda + q_1, \tag{3.4}$$

where
$p_1 = 2 + (\tau^* + \delta)(1 - 2x^* - \frac{ak_1y^*}{(x^*+k_1)^2} - c)$,
$q_1 = (-1+c\delta+c\tau^*)[2x^*(\tau^*+\delta)-(1+\tau^*+\delta)]+\frac{ac(\tau^*+\delta)^2x^*}{k_1+x^*}+\frac{ak_1(\tau^*+\delta)(-1+c(\tau^*+\delta))y^*}{(k_1+x^*)^2}$.
The transversal condition with respect to $E_*(x^*, y^*)$ is

$$\left.\frac{dg(\lambda)}{d\delta}\right|_{\lambda=-1,\delta=0} = 2-2c-4x^*-\frac{2ak_1y^*}{(k_1+x^*)^2}+2c\tau^*(-1+x^*(2+\frac{a}{k_1+x^*})+\frac{ak_1y^*}{(k_1+x^*)^2}).$$

If $\left.\frac{dg(\lambda)}{d\delta}\right|_{\lambda=-1,\delta=0} \neq 0$, then Flip bifurcation will appear around $E_*(x^*, y^*)$.

3.1.2. The direction of Flip bifurcation at $E_*(x^*, y^*)$

To facilitate discussion, define

$$A = \begin{pmatrix} 1 + \tau^*[1 - 2x^* - \frac{ak_1y^*}{(x^*+k_1)^2}] & -\frac{a\tau^*x^*}{x^*+k_1} \\ c\tau^* & 1 - c\tau^* \end{pmatrix},$$

If the eigenvalue of A goes for $\lambda = -1$, the corresponding eigenvector is given as:

$$\xi_1 = \begin{pmatrix} \frac{a\tau^*x^*}{x^*+k_1} \\ 2 + \tau^*(1 - 2x^* - \frac{ay^*k_1}{(x^*+k_1)^2}) \end{pmatrix}.$$

If the eigenvalue of A goes for $\lambda = \lambda_2$, the corresponding eigenvector is given as:

$$\xi_2 = \begin{pmatrix} \frac{a\tau^* x^*}{x^*+k_1} \\ 1-\lambda_2+\tau^*(1-2x^*-\frac{ay^*k_1}{(x^*+k_1)^2}) \end{pmatrix}.$$

Then we have the invertible matrix

$$T = (\xi_1\ \xi_2) = \begin{pmatrix} \frac{a\tau^* x^*}{x^*+k_1} & \frac{a\tau^* x^*}{x^*+k_1} \\ 2+\tau^*(1-2x^*-\frac{ay^*k_1}{(x^*+k_1)^2}) & 1-\lambda_2+\tau^*(1-2x^*-\frac{ay^*k_1}{(x^*+k_1)^2}) \end{pmatrix},$$

and its inverse matrix

$$T^{-1} = \begin{pmatrix} \frac{(x^*+k_1)(-1-\tau^*(1-2x^*-\frac{ay^*k_1}{(x^*+k_1)^2})+\lambda_2)}{a\tau^* x^*(1+\lambda_2)} & \frac{1}{1+\lambda_2} \\ \frac{(x^*+k_1)(2+\tau^*(1-2x^*-\frac{ay^*k_1}{(x^*+k_1)^2}))}{a\tau^* x^*(1+\lambda_2)} & -\frac{1}{1+\lambda_2} \end{pmatrix}.$$

We use the translation

$$\begin{pmatrix} X_{n+1} \\ Y_{n+1} \end{pmatrix} = T \begin{pmatrix} u_{n+1} \\ v_{n+1} \end{pmatrix},$$

then system (3.3) can be changed into

$$\begin{pmatrix} u_{n+1} \\ v_{n+1} \end{pmatrix} = \begin{pmatrix} -1 & 0 \\ 0 & \lambda_2 \end{pmatrix} \begin{pmatrix} u_n \\ v_n \end{pmatrix} + \begin{pmatrix} f_1(X_n, Y_n, \delta) \\ g_1(X_n, Y_n, \delta) \end{pmatrix}, \tag{3.5}$$

where

$$\begin{aligned} f_1(X_n, Y_n, \delta) &= B_{11}X\delta + B_{12}Y\delta + C_{11}X^2 + C_{12}XY + C_{13}Y^2 + C_{14}X^3 + C_{15}X^2Y + C_{16}XY^2 \\ &\quad + C_{17}Y^3 + D_{11}X^2\delta + D_{12}XY\delta + D_{13}Y^2\delta + O((|X|+|Y|+|\delta|)^4), \\ g_1(X_n, Y_n, \delta) &= B_{21}X\delta + B_{22}Y\delta + C_{21}X^2 + C_{22}XY + C_{23}Y^2 + C_{24}X^3 + C_{25}X^2Y + C_{26}XY^2 \\ &\quad + C_{27}Y^3 + D_{21}X^2\delta + D_{22}XY\delta + D_{23}Y^2\delta + O((|X|+|Y|+|\delta|)^4), \end{aligned}$$

$B_{11} = \frac{c}{1+\lambda_2} + \frac{(1-2x^*-\frac{ak_1y^*}{(k_1+x^*)^2})(-1+\lambda_2-\tau^*(1-2x^*-\frac{ak_1y^*}{(k_1+x^*)^2}))(k_1+x^*)}{a(1+\lambda_2)\tau^* x^*}$, $B_{12} = -\frac{c}{1+\lambda_2} - \frac{-1+\lambda_2-\tau^*(1-2x^*-\frac{ak_1y^*}{(k_1+x^*)^2})}{(1+\lambda_2)\tau^*}$, $C_{11} = \frac{-c\tau^* {y^*}^2}{(1+\lambda_2)(k_2+x^*)^3} + \frac{(-1+\frac{ak_1y^*}{(k_1+x^*)^3})(-1+\lambda_2-\tau^*(1-2x^*-\frac{ak_1y^*}{(k_1+x^*)^2}))(k_1+x^*)}{a(1+\lambda_2)x^*}$,

$C_{12} = \frac{2c\tau^* y^*}{(1+\lambda_2)(k_2+x^*)^2} - \frac{k_1(-1+\lambda_2-\tau^*(1-2x^*-\frac{ak_1y^*}{(k_1+x^*)^2}))}{(1+\lambda_2)x^*(k_1+x^*)}$, $C_{13} = -\frac{c\tau^*}{(1+\lambda_2)(k_2+x^*)}$, $C_{14} = \frac{c\tau^* {y^*}^2}{(1+\lambda_2)(k_2+x^*)^4} - \frac{k_1 y^*(-1+\lambda_2-\tau^*(1-2x^*-\frac{ak_1y^*}{(k_1+x^*)^2}))}{(1+\lambda_2)x^*(k_1+x^*)^3}$, $C_{15} = \frac{-2c\tau^* y^*}{(1+\lambda_2)(k_2+x^*)^3} + \frac{k_1(-1+\lambda_2-\tau^*(1-2x^*-\frac{ak_1y^*}{(k_1+x^*)^2}))}{(1+\lambda_2)x^*(k_1+x^*)^2}$,

$C_{16} = \frac{c\tau^*}{(1+\lambda_2)(k_2+x^*)^2}$, $C_{17} = 0$, $D_{11} = \frac{-c{y^*}^2}{(1+\lambda_2)(k_2+x^*)^3} + \frac{(k_1+x^*)(-1+\frac{ak_1y^*}{(k_1+x^*)^3})(-1+\lambda_2-\tau^*(1-2x^*-\frac{ak_1y^*}{(k_1+x^*)^2}))}{a(1+\lambda_2)x^*\tau^*}$,

$D_{12} = \frac{2cy^*}{(1+\lambda_2)(k_2+x^*)^2} - \frac{k_1(-1+\lambda_2-\tau^*(1-2x^*-\frac{ak_1y^*}{(k_1+x^*)^2}))}{(1+\lambda_2)x^*\tau^*(k_1+x^*)}$, $D_{13} = -\frac{c}{(1+\lambda_2)(k_2+x^*)}$, $B_{21} = -\frac{c}{1+\lambda_2} + \frac{(1-2x^*-\frac{ak_1y^*}{(k_1+x^*)^2})(2+\tau^*(1-2x^*-\frac{ak_1y^*}{(k_1+x^*)^2}))(k_1+x^*)}{a(1+\lambda_2)\tau^* x^*}$, $B_{22} = \frac{c}{1+\lambda_2} - \frac{2+\tau^*(1-2x^*-\frac{ak_1y^*}{(k_1+x^*)^2})}{(1+\lambda_2)\tau^*}$,

$C_{21} = \frac{c\tau^* {y^*}^2}{(1+\lambda_2)(k_2+x^*)^3} + \frac{(k_1+x^*)(-1+\frac{ak_1y^*}{(k_1+x^*)^3})(2+\tau^*(1-2x^*-\frac{ak_1y^*}{(k_1+x^*)^2}))}{a(1+\lambda_2)x^*}$, $C_{22} = \frac{-2c\tau^* y^*}{(1+\lambda_2)(k_2+x^*)^2} -$

$\frac{k_1(2+\tau^*(1-2x^*-\frac{ak_1y^*}{(k_1+x^*)^2}))}{(1+\lambda_2)x^*(k_1+x^*)}$, $C_{23}=\frac{c\tau^*}{(1+\lambda_2)(k_2+x^*)}$, $C_{24}=-\frac{c\tau^*{y^*}^2}{(1+\lambda_2)(k_2+x^*)^4}-\frac{k_1y^*(2+\tau^*(1-2x^*-\frac{ak_1y^*}{(k_1+x^*)^2}))}{(1+\lambda_2)x^*(k_1+x^*)^3}$,
$C_{25}=\frac{2c\tau^*y^*}{(1+\lambda_2)(k_2+x^*)^3}+\frac{k_1(2+\tau^*(1-2x^*-\frac{ak_1y^*}{(k_1+x^*)^2}))}{(1+\lambda_2)x^*(k_1+x^*)^2}$, $C_{26}=\frac{-c\tau^*}{(1+\lambda_2)(k_2+x^*)^2}$, $C_{27}=0$,
$D_{21}=\frac{c{y^*}^2}{(1+\lambda_2)(k_2+x^*)^3}+\frac{(k_1+x^*)(-1+\frac{ak_1y^*}{(k_1+x^*)^3})(2+\tau^*(1-2x^*-\frac{ak_1y^*}{(k_1+x^*)^2}))}{a(1+\lambda_2)\tau^*x^*}$, $D_{22}=\frac{-2cy^*}{(1+\lambda_2)(k_2+x^*)^2}-$
$\frac{k_1(2+\tau^*(1-2x^*-\frac{ak_1y^*}{(k_1+x^*)^2}))}{(1+\lambda_2)\tau^*x^*(k_1+x^*)}$, $D_{23}=\frac{c}{(1+\lambda_2)(k_2+x^*)}$.

To facilitate calculation, we set

$$T=\begin{pmatrix}\frac{a\tau^*x^*}{x^*+k_1} & \frac{a\tau^*x^*}{x^*+k_1}\\ 2+\tau^*(1-2x^*-\frac{ay^*k_1}{(x^*+k_1)^2}) & 1-\lambda_2+\tau^*(1-2x^*-\frac{ay^*k_1}{(x^*+k_1)^2})\end{pmatrix}=\begin{pmatrix}t_{11} & t_{12}\\ t_{21} & t_{22}\end{pmatrix}.$$

Using translation $\begin{pmatrix}X_n\\ Y_n\end{pmatrix}=T\begin{pmatrix}u_n\\ v_n\end{pmatrix}$, system (3.5) becomes

$$\begin{pmatrix}u_{n+1}\\ v_{n+1}\end{pmatrix}=\begin{pmatrix}-1 & 0\\ 0 & \lambda_2\end{pmatrix}\begin{pmatrix}u_n\\ v_n\end{pmatrix}+\begin{pmatrix}f_2(u_n,v_n,\delta)\\ g_2(u_n,v_n,\delta)\end{pmatrix},\tag{3.6}$$

where

$f_2(u_n,v_n,\delta)=m_{11}u_n\delta+m_{12}v_n\delta+m_{13}u_n^2+m_{14}u_nv_n+m_{15}v_n^2+m_{16}u_n^3+m_{17}u_n^2v_n+m_{18}u_nv_n^2+m_{19}v_n^3+q_{11}u_n^2\delta+q_{12}v_n^2\delta+q_{13}u_nv_n\delta+O((|u_n|+|v_n|+|\delta|)^4)$,
$g_2(u_n,v_n,\delta)=m_{21}u_n\delta+m_{22}v_n\delta+m_{23}u_n^2+m_{24}u_nv_n+m_{25}v_n^2+m_{26}u_n^3+m_{27}u_n^2v_n+m_{28}u_nv_n^2+m_{29}v_n^3+q_{21}u_n^2\delta+q_{22}v_n^2\delta+q_{23}u_nv_n\delta+O((|u_n|+|v_n|+|\delta|)^4)$,
$m_{11}=B_{11}t_{11}+B_{12}t_{21}, m_{12}=B_{11}t_{12}+B_{12}t_{22}, m_{13}=C_{11}{t_{11}}^2+C_{12}t_{11}t_{21}+C_{13}{t_{21}}^2, m_{14}=2C_{11}t_{11}t_{12}+C_{12}t_{12}t_{21}+C_{12}t_{11}t_{22}+2C_{13}t_{21}t_{22}, m_{15}=C_{11}{t_{12}}^2+C_{12}t_{12}t_{22}+C_{13}{t_{22}}^2, m_{16}=C_{14}{t_{11}}^3+C_{15}{t_{11}}^2t_{21}+C_{16}t_{11}{t_{21}}^2+C_{17}{t_{21}}^3, m_{17}=3C_{14}{t_{11}}^2t_{12}+2C_{15}t_{11}t_{12}t_{21}+C_{16}t_{12}{t_{21}}^2+C_{15}{t_{11}}^2t_{22}+2C_{16}t_{11}t_{21}t_{22}+3C_{17}{t_{21}}^2t_{22}, m_{18}=3C_{14}t_{11}{t_{12}}^2+2C_{15}t_{11}t_{12}t_{22}+C_{16}t_{11}{t_{22}}^2+C_{15}{t_{12}}^2t_{21}+2C_{16}t_{12}t_{21}t_{22}+3C_{17}t_{21}{t_{22}}^2, m_{19}=C_{14}{t_{12}}^3+C_{15}{t_{12}}^2t_{22}+C_{16}t_{12}{t_{22}}^2+C_{17}{t_{22}}^3, q_{11}=D_{11}{t_{11}}^2+D_{12}t_{11}t_{21}+D_{13}{t_{21}}^2, q_{12}=D_{11}{t_{12}}^2+D_{12}t_{12}t_{22}+D_{13}{t_{22}}^2, q_{13}=2D_{11}t_{11}t_{12}+D_{12}t_{12}t_{21}+D_{12}t_{11}t_{22}+2D_{13}t_{21}t_{22}$,
$m_{21}=B_{21}t_{11}+B_{22}t_{21}, m_{22}=B_{21}t_{12}+B_{22}t_{22}, m_{23}=C_{21}{t_{11}}^2+C_{22}t_{11}t_{21}+C_{23}{t_{21}}^2, m_{24}=2C_{21}t_{11}t_{12}+C_{22}t_{12}t_{21}+C_{22}t_{11}t_{22}+2C_{23}t_{21}t_{22}, m_{25}=C_{21}{t_{12}}^2+C_{22}t_{12}t_{22}+C_{23}{t_{22}}^2, m_{26}=C_{24}{t_{11}}^3+C_{25}{t_{11}}^2t_{21}+C_{26}t_{11}{t_{21}}^2+C_{27}{t_{21}}^3, m_{27}=3C_{24}{t_{11}}^2t_{12}+2C_{25}t_{11}t_{12}t_{21}+C_{26}t_{12}{t_{21}}^2+C_{25}{t_{11}}^2t_{22}+2C_{26}t_{11}t_{21}t_{22}+3C_{27}{t_{21}}^2t_{22}, m_{28}=3C_{24}t_{11}{t_{12}}^2+2C_{25}t_{11}t_{12}t_{22}+C_{26}t_{11}{t_{22}}^2+C_{25}{t_{12}}^2t_{21}+2C_{26}t_{12}t_{21}t_{22}+3C_{27}t_{21}{t_{22}}^2, m_{29}=C_{24}{t_{12}}^3+C_{25}{t_{12}}^2t_{22}+C_{26}t_{12}{t_{22}}^2+C_{27}{t_{22}}^3, q_{21}=D_{21}{t_{11}}^2+D_{22}t_{11}t_{21}+D_{23}{t_{21}}^2, q_{22}=D_{21}{t_{12}}^2+D_{22}t_{12}t_{22}+D_{23}{t_{22}}^2, q_{23}=2D_{21}t_{11}t_{12}+D_{22}t_{12}t_{21}+D_{22}t_{11}t_{22}+2D_{23}t_{21}t_{22}$.

The central manifold theorem [34, 35] claims that there exists a three-dimensional central manifold $W^c(0)$:

$$W^c{}_{loc}(0)=\left\{(u_n,v_n,\delta)\in R^3: v_n=h(u_n,\delta)=z_1{u_n}^2+z_2u_n\delta+z_3\delta^2+O((|u_n|+|\delta|)^3)\right\},$$

and must satisfy the following quasilinear partial difference equation:

$$N(h(x))=h(-u_n+f_2(u_n,h(u_n,\delta),\delta),\delta)-\lambda_2h(u_n,\delta)-g_2(u_n,h(u_n,\delta),\delta)=0,$$

where u_n and δ sufficiently small.

It can be obtained by balancing powers of coefficients for each component:

$$z_1=\frac{m_{23}}{1-\lambda_2}=\frac{C_{21}{t_{11}}^2+C_{22}t_{11}t_{21}+C_{23}{t_{21}}^2}{1-\lambda_2}, z_2=-\frac{m_{21}}{1+\lambda_2}=-\frac{B_{21}t_{11}+B_{22}t_{21}}{1+\lambda_2}, z_3=0.$$

Hence the system restricted to the central manifold $W^c{}_{loc}(0)$ is expressed by:

$$F: u_{n+1} = -u_n + \vartheta_1 {u_n}^2 + \vartheta_2 u_n\delta + \vartheta_3 {u_n}^2\delta + \vartheta_4 u_n\delta^2 + \vartheta_5 {u_n}^3 + O((|u_n| + |\delta|)^4),$$

where
$\vartheta_1 = m_{13} = C_{11}{t_{11}}^2 + C_{12}t_{11}t_{21} + C_{13}{t_{21}}^2, \vartheta_2 = m_{11} = B_{11}t_{11} + B_{12}t_{21}, \vartheta_3 = m_{12}z_1 + m_{14}z_2 = (B_{11}t_{12} + B_{12}t_{22})\frac{C_{21}{t_{11}}^2 + C_{22}t_{11}t_{21} + C_{23}{t_{21}}^2}{1-\lambda_2} - (2C_{11}t_{11}t_{12} + C_{12}t_{12}t_{21} + C_{12}t_{11}t_{22} + 2C_{13}t_{21}t_{22})\frac{B_{21}t_{11} + B_{22}t_{21}}{1+\lambda_2}, \vartheta_4 = m_{12}z_2 = -(B_{11}t_{12} + B_{12}t_{22})\frac{B_{21}t_{11} + B_{22}t_{21}}{1+\lambda_2}, \vartheta_5 = m_{16} + m_{14}z_1 = C_{14}{t_{11}}^3 + C_{15}{t_{11}}^2t_{21} + C_{16}t_{11}{t_{21}}^2 + C_{17}{t_{21}}^3 + (2C_{11}t_{11}t_{12} + C_{12}t_{12}t_{21} + C_{12}t_{11}t_{22} + 2C_{13}t_{21}t_{22})\frac{C_{21}{t_{11}}^2 + C_{22}t_{11}t_{21} + C_{23}{t_{21}}^2}{1-\lambda_2}$.
Then we need to calculate the following two coefficients at $(u, v, \delta) = (0, 0, 0)$:

$$\alpha_1 = \left(\frac{\partial^2 F}{\partial u_n \partial\delta} + \frac{1}{2}\frac{\partial F}{\partial\delta}\frac{\partial^2 F}{\partial {u_n}^2}\right)\Big|_{(0,0)} = \vartheta_2, \ \alpha_2 = \left(\frac{1}{6}\frac{\partial^3 F}{\partial {u_n}^3} + (\frac{1}{2}\frac{\partial^2 F}{\partial {u_n}^2})^2\right)\Big|_{(0,0)} = \vartheta_5 + {\vartheta_1}^2.$$

We can get the following theorem:

Theorem 3.1. *If $\alpha_1 \neq 0$, $\alpha_2 \neq 0$, then the model (1.5) undergoes a Flip bifurcation at the positive equilibrium point $E_*(x^*, y^*)$ when parameter τ fluctuates within a small region of U_1. Furthermore, when $\alpha_2 > 0$(resp., $\alpha_2 < 0$), model (1.5) bifurcates into a periodic two stable(resp.,unstable) orbit from the positive equilibrium $E_*(x^*, y^*)$.*

3.2. Hopf bifurcation at $E_*(x^*, y^*)$

Next, we study the Hopf bifurcation of $E_*(x^*, y^*)$ of model (1.5) and still select τ as the bifurcation parameter. The following curve determines the essential condition for Hopf bifurcation to occur:
$N.S = \left\{(a, c, k_1, k_2, \tau) \in {R_+}^5 : \tau = {\tau_1}^* = \frac{(-1+c+\alpha+\beta)(\alpha+\beta+2k_1)^2 + 2ak_1(\alpha+\beta+2k_2)}{c[(\alpha+\beta)^2(-1+a+\alpha+\beta) + 4(-1+\alpha+\beta){k_1}^2 + 4k_1((\alpha+\beta)(-1+a+\alpha+\beta) + ak_2)]}\right\}$,

3.2.1. Existence condition of Hopf bifurcation at $E_*(x^*, y^*)$

According to (A_5) in Theorem (2.4), we can easily obtain the bifurcation parameter ${\tau_1}^* = \frac{(-1+c+\alpha+\beta)(\alpha+\beta+2k_1)^2 + 2ak_1(\alpha+\beta+2k_2)}{c[(\alpha+\beta)^2(-1+a+\alpha+\beta) + 4(-1+\alpha+\beta){k_1}^2 + 4k_1((\alpha+\beta)(-1+a+\alpha+\beta) + ak_2)]}$. We still consider parameter τ with a small perturbation δ, and then the corresponding characteristic equation can be written as:

$$\lambda^2 + p(\delta)\lambda + q(\delta) = 0,$$

where
$p(\delta) = -[2 + ({\tau_1}^* + \delta)(1 - 2x^* - \frac{ak_1y^*}{(x^*+k_1)^2} - c)]$,
$q(\delta) = (-1+c({\tau_1}^*+\delta))[2x^*({\tau_1}^*+\delta) - (1+{\tau_1}^*+\delta)] + \frac{acx^*({\tau_1}^*+\delta)^2}{k_1+x^*} + \frac{ak_1y^*({\tau_1}^*+\delta)(-1+c({\tau_1}^*+\delta))}{(k_1+x^*)^2}$.
Since parameters $(a, c, k_1, k_2, \tau) \in N.S$, the roots of the characteristic equation are

$$\lambda_{1,2} = \frac{-p(\delta) \pm i\sqrt{4q(\delta) - p(\delta)^2}}{2},$$

and we have

$$|\lambda_{1,2}| = \sqrt{q(\delta)},$$

$$\left.\frac{d\,|\lambda_{1,2}|}{d\delta}\right|_{\delta=0} = \frac{1-c-2c{\tau_1}^*+x^*(-2+2c{\tau_1}^*(2+\frac{a}{k_1+x^*}))+\frac{a(-1+2c{\tau_1}^*)k_1y^*}{(k_1+x^*)^2}}{2\sqrt{\frac{ac{\tau_1}^{*2}x^*}{k_1+x^*}+(-1+c{\tau_1}^*)(-1-{\tau_1}^*+2{\tau_1}^*x^*)+\frac{a{\tau_1}^*(-1+c{\tau_1}^*)k_1y^*}{(k_1+x^*)^2}}}.$$

The occurence of Hopf bifurcation requires the following conditions [36]:
$(E.1)$ $\left.\frac{d|\lambda_{1,2}|}{d\delta}\right|_{\delta=0} \neq 0$;
$(E.2)$ ${\lambda_{1,2}}^i \neq 1$ *when* $\delta = 0,\ i = 1,2,3,4.$
Obviously, $(E.1)$ is identical to the following expression hold:

$$1-2c{\tau_1}^*-c+x^*(-2+2c{\tau_1}^*(2+\frac{a}{k_1+x^*}))+\frac{a(-1+2c{\tau_1}^*)k_1y^*}{(k_1+x^*)^2}\neq 0,$$

which means that

$${\tau_1}^* \neq \frac{-1+c+2x^*+\frac{ak_1y^*}{(x^*+k_1)^2}}{-2c+\frac{2ack_1y^*}{(x^*+k_1)^2}+2cx^*(2+\frac{a}{x^*+k_1})}.$$

In addition, $(E.2)$ is identical to $p(0)\neq -2,0,1,2$. Since $|p(0)|<2$, the condition becomes $p(0)\neq 0,1$, so we have

$${\tau_1}^* \neq \frac{2}{-1+c+2x^*+\frac{ak_1y^*}{(k_1+x^*)^2}}, and\ \ {\tau_1}^* \neq \frac{3}{-1+c+2x^*+\frac{ak_1y^*}{(k_1+x^*)^2}}.$$

3.2.2. The direction of Hopf bifurcation at $E_*(x^*,y^*)$

Let

$$\mu = -\frac{p(0)}{2} = \frac{2+{\tau_1}^*(1-2x^*-\frac{ak_1y^*}{(x^*+k_1)^2}-c)}{2},$$

$$\omega = \frac{\sqrt{4q(0)-p(0)^2}}{2}$$

$$= \frac{1}{2}\sqrt{4(\frac{ac{\tau_1}^{*2}x^*}{k_1+x^*}+(-1+c{\tau_1}^*)(-1-{\tau_1}^*+2{\tau_1}^*x^*)+\frac{a{\tau_1}^*(-1+c{\tau_1}^*)k_1y^*}{(k_1+x^*)^2})-(2+{\tau_1}^*(1-c-2x^*-\frac{ak_1y^*}{(k_1+x^*)^2}))^2}.$$

The invertible matrix T_1 can be expressed as

$$T_1 = \begin{pmatrix} \frac{a{\tau_1}^*x^*}{x^*+k_1} & 0 \\ 3\mu-1+c{\tau_1}^* & \omega \end{pmatrix},$$

we use the following transformation:

$$\begin{pmatrix} \bar{X}_{n+1} \\ \bar{Y}_{n+1} \end{pmatrix} = T_1 \begin{pmatrix} \bar{u}_{n+1} \\ \bar{v}_{n+1} \end{pmatrix},$$

and then the system (3.3) transforms to

$$\begin{pmatrix} \bar{u}_{n+1} \\ \bar{v}_{n+1} \end{pmatrix} = \begin{pmatrix} \mu & -\omega \\ \omega & \mu \end{pmatrix} \begin{pmatrix} \bar{u}_n \\ \bar{v}_n \end{pmatrix} + \begin{pmatrix} f(\bar{X}_n,\bar{Y}_n) \\ g(\bar{X}_n,\bar{Y}_n) \end{pmatrix}, \tag{3.7}$$

where

$f(\bar{X}_n,\bar{Y}_n)=l_{11}\bar{X}_n^2+l_{12}\bar{X}_n\bar{Y}_n+l_{13}\bar{Y}_n^2+l_{14}\bar{X}_n^3+l_{15}\bar{X}_n^2\bar{Y}_n+l_{16}\bar{X}_n\bar{Y}_n^2+l_{17}\bar{Y}_n^3+O((|\bar{X}_n|+|\bar{Y}_n|)^4)$,
$g(\bar{X}_n,\bar{Y}_n)=l_{21}\bar{X}_n^2+l_{22}\bar{X}_n\bar{Y}_n+l_{23}\bar{Y}_n^2+l_{24}\bar{X}_n^3+l_{25}\bar{X}_n^2\bar{Y}_n+l_{26}\bar{X}_n\bar{Y}_n^2+l_{27}\bar{Y}_n^3+O((|\bar{X}_n|+|\bar{Y}_n|)^4)$,
$l_{11}=\frac{k_1+x^*}{a{\tau_1}^*x^*}(-1+\frac{ak_1y^*}{(k_1+x^*)^3}), l_{12}=\frac{k_1+x^*}{a{\tau_1}^*x^*}(-\frac{ak_1}{(k_1+x^*)^2}), l_{13}=0, l_{14}=\frac{k_1+x^*}{a{\tau_1}^*x^*}(-\frac{ak_1y^*}{(k_1+x^*)^4}), l_{15}=\frac{k_1+x^*}{a{\tau_1}^*x^*}(\frac{ak_1}{(k_1+x^*)^3}), l_{16}=0, l_{17}=0, l_{21}=\frac{(k_1+x^*)(1-3\mu-c{\tau_1}^*)}{a\omega{\tau_1}^*x^*}(-1+\frac{ak_1y^*}{(k_1+x^*)^3})-\frac{c{y^*}^2}{\omega(k_2+x^*)^3}, l_{22}=\frac{(k_1+x^*)(1-3\mu-c{\tau_1}^*)}{a\omega{\tau_1}^*x^*}(-\frac{ak_1}{(k_1+x^*)^2})+\frac{2cy^*}{\omega(k_2+x^*)^2}, l_{23}=-\frac{c}{\omega(k_2+x^*)}, l_{24}=\frac{(k_1+x^*)(1-3\mu-c{\tau_1}^*)}{a\omega{\tau_1}^*x^*}(-\frac{ak_1y^*}{(k_1+x^*)^4})+\frac{c{y^*}^2}{\omega(k_2+x^*)^4}, l_{25}=\frac{(k_1+x^*)(1-3\mu-c{\tau_1}^*)}{a\omega{\tau_1}^*x^*}(\frac{ak_1}{(k_1+x^*)^3})-\frac{2cy^*}{\omega(k_2+x^*)^3}, l_{26}=\frac{c}{\omega(k_2+x^*)^2}, l_{27}=0,$
and we use the translation

$$\begin{pmatrix}\bar{X}_n\\ \bar{Y}_n\end{pmatrix}=T_1\begin{pmatrix}\bar{u}_n\\ \bar{v}_n\end{pmatrix},$$

i.e., $\bar{X}_n=\frac{a{\tau_1}^*x^*}{x^*+k_1}\bar{u}_n, \bar{Y}_n=(3\mu-1+c{\tau_1}^*)\bar{u}_n+\omega\bar{v}_n$, and then the system (3.7) transforms to

$$\begin{pmatrix}\bar{u}_{n+1}\\ \bar{v}_{n+1}\end{pmatrix}=\begin{pmatrix}\mu & -\omega\\ \omega & \mu\end{pmatrix}\begin{pmatrix}\bar{u}_n\\ \bar{v}_n\end{pmatrix}+\begin{pmatrix}\tilde{f}(\bar{u}_n,\bar{v}_n)\\ \tilde{g}(\bar{u}_n,\bar{v}_n)\end{pmatrix},\tag{3.8}$$

where

$\tilde{f}(\bar{u}_n,\bar{v}_n)=p_{11}\bar{u}_n^2+p_{12}\bar{u}_n\bar{v}_n+p_{13}\bar{v}_n^2+p_{14}\bar{u}_n^3+p_{15}\bar{u}_n^2\bar{v}_n+p_{16}\bar{u}_n\bar{v}_n^2+p_{17}\bar{v}_n^3+O((|\bar{u}_n|+|\bar{v}_n|)^4)$,
$\tilde{g}(\bar{u}_n,\bar{v}_n)=p_{21}\bar{u}_n^2+p_{22}\bar{u}_n\bar{v}_n+p_{23}\bar{v}_n^2+p_{24}\bar{u}_n^3+p_{25}\bar{u}_n^2\bar{v}_n+p_{26}\bar{u}_n\bar{v}_n^2+p_{27}\bar{v}_n^3+O((|\bar{u}_n|+|\bar{v}_n|)^4)$,
$p_{11}=\frac{{a\tau_1}^{*2}x^{*2}l_{11}}{(k_1+x^*)^2}+\frac{a{\tau_1}^*x^*l_{12}(-1+3\mu+c{\tau_1}^*)}{k_1+x^*}, p_{12}=\frac{\omega a{\tau_1}^*x^*l_{12}}{k_1+x^*}, p_{13}=0, p_{14}=\frac{{a\tau_1}^{*3}x^{*3}l_{14}}{(k_1+x^*)^3}+\frac{{a\tau_1}^{*2}x^{*2}l_{15}(-1+3\mu+c{\tau_1}^*)}{(k_1+x^*)^2}, p_{15}=\frac{\omega{a\tau_1}^{*2}x^{*2}l_{15}}{(k_1+x^*)^2}, p_{16}=0, p_{17}=0,$
$p_{21}=(-1+3\mu+c{\tau_1}^*)^2l_{23}+\frac{{a\tau_1}^{*2}x^{*2}l_{21}}{(k_1+x^*)^2}+\frac{a{\tau_1}^*x^*l_{22}(-1+3\mu+c{\tau_1}^*)}{k_1+x^*}, p_{22}=2\omega(-1+3\mu+c{\tau_1}^*)l_{23}+\frac{\omega a{\tau_1}^*x^*l_{22}}{k_1+x^*}, p_{23}=\omega^2l_{23}, p_{24}=\frac{{a\tau_1}^{*3}x^{*3}l_{24}}{(k_1+x^*)^3}+\frac{{a\tau_1}^{*2}x^{*2}l_{25}(-1+3\mu+c{\tau_1}^*)}{(k_1+x^*)^2}+\frac{a{\tau_1}^*x^*l_{26}(-1+3\mu+c{\tau_1}^*)^2}{k_1+x^*}, p_{25}=\frac{\omega{a\tau_1}^{*2}x^{*2}l_{25}}{(k_1+x^*)^2}+\frac{2\omega a{\tau_1}^*x^*l_{26}(-1+3\mu+c{\tau_1}^*)}{k_1+x^*}, p_{26}=\frac{\omega^2a{\tau_1}^*x^*l_{26}}{k_1+x^*}, p_{27}=0.$

To decide the stability of the invariant circle bifurcated from Hopf bifurcation of the model (3.8), we are supposed to compute the discriminating coefficient a^* [37], which is expressed as:

$$a^*=-\mathrm{Re}[\frac{(1-2\lambda)\bar{\lambda}^2}{1-\lambda}L_{11}L_{20}]-\frac{1}{2}|L_{11}|^2-|L_{02}|^2+\mathrm{Re}(\bar{\lambda}L_{21}),$$

where

$$L_{20}=\frac{1}{8}[(\tilde{f}_{\bar{u}\bar{u}}-\tilde{f}_{\bar{v}\bar{v}}+2\tilde{g}_{\bar{u}\bar{v}})+i(\tilde{g}_{\bar{u}\bar{u}}-\tilde{g}_{\bar{v}\bar{v}}-2\tilde{f}_{\bar{u}\bar{v}})],$$
$$L_{11}=\frac{1}{4}[(\tilde{f}_{\bar{u}\bar{u}}+\tilde{f}_{\bar{v}\bar{v}})+i(\tilde{g}_{\bar{u}\bar{u}}+\tilde{g}_{\bar{v}\bar{v}})],$$
$$L_{02}=\frac{1}{8}[(\tilde{f}_{\bar{u}\bar{u}}-\tilde{f}_{\bar{v}\bar{v}}-2\tilde{g}_{\bar{u}\bar{v}})+i(\tilde{g}_{\bar{u}\bar{u}}-\tilde{g}_{\bar{v}\bar{v}}+2\tilde{f}_{\bar{u}\bar{v}})],$$

$$L_{21} = \frac{1}{16}[(\tilde{f}_{\bar{u}\bar{u}\bar{u}} + \tilde{f}_{\bar{u}\bar{v}\bar{v}} + \tilde{g}_{\bar{u}\bar{u}\bar{v}} + \tilde{g}_{\bar{v}\bar{v}\bar{v}}) + i(\tilde{g}_{\bar{u}\bar{u}\bar{u}} + \tilde{g}_{\bar{u}\bar{v}\bar{v}} - \tilde{f}_{\bar{u}\bar{u}\bar{v}} - \tilde{f}_{\bar{v}\bar{v}\bar{v}})].$$

Some computations produce that

$$\tilde{f}_{\bar{u}\bar{u}}\Big|_{(0,0)} = 2p_{11},\ \tilde{f}_{\bar{u}\bar{v}}\Big|_{(0,0)} = p_{12},\ \tilde{f}_{\bar{u}\bar{u}\bar{u}}\Big|_{(0,0)} = 6p_{14},\ \tilde{f}_{\bar{u}\bar{u}\bar{v}}\Big|_{(0,0)} = 2p_{15},$$

$$\tilde{f}_{\bar{u}\bar{v}\bar{v}}\Big|_{(0,0)} = 2p_{16},\ \tilde{f}_{\bar{v}\bar{v}}\Big|_{(0,0)} = 2p_{13},\ \tilde{f}_{\bar{v}\bar{v}\bar{v}}\Big|_{(0,0)} = 6p_{17},$$

$$\tilde{g}_{\bar{u}\bar{u}}|_{(0,0)} = 2p_{21},\ \tilde{g}_{\bar{u}\bar{v}}|_{(0,0)} = p_{22},\ \tilde{g}_{\bar{u}\bar{u}\bar{u}}|_{(0,0)} = 6p_{24},\ \tilde{g}_{\bar{u}\bar{u}\bar{v}}|_{(0,0)} = 2p_{25},$$

$$\tilde{g}_{\bar{u}\bar{v}\bar{v}}|_{(0,0)} = 2p_{26},\ \tilde{g}_{\bar{v}\bar{v}}|_{(0,0)} = 2p_{23},\ \tilde{g}_{\bar{v}\bar{v}\bar{v}}|_{(0,0)} = 6p_{27}.$$

Assume that the transversal condition $(E.1)$ and the non-degenerate condition $(E.2)$ of the model (1.5) are satisfied when parameter τ varies in the small region of ${\tau_1}^*$ in the set of N.S. The following theorem holds:

Theorem 3.2. *If $a^* \neq 0$, then the system (1.5) undergoes a Hopf bifurcation around the positive point $E_*(x^*, y^*)$ when the parameter τ fluctuates within the small region of ${\tau_1}^*$ in the set of N.S. Furthermore, if $a^* < 0$(resp.,$a^* > 0$), an attracting(resp., repelling) invariant closed curve bifurcates from the point $E_*(x^*, y^*)$ for $\tau > {\tau_1}^*$ (resp., $\tau < {\tau_1}^*$).*

4. Numerical simulations

In this section, the previous theoretical results will be analysed with the help of numerical simulations to show the dynamical behaviour of the model (1.5) around the unique positive equilibrium $E_*(x^*, y^*)$.

4.1. Numerical simulation of Flip bifurcation

Firstly, we choose τ as the bifurcation parameter in curve U_1 to study the dynamical properties of system (1.5) at $E_*(x^*, y^*)$. We choose the following parameters to discuss.

The unique positive equilibrium point $(x_0, y_0) \approx (0.3, 0.46666667)$ of the model can be obtained by giving the parameters

$$\tau \approx 2.22222222222, r = 0.1, s = 0.18, m = 0.35, n = 0.8, z = 0.3, K = 2, K_2 = 0.1.$$

Then we can easily get the corresponding parameters in system (1.5):

$$a = 1.05, c = 1.8, k_1 = 0.4, k_2 = 0.16666667.$$

By choosing the initial value of $(\tilde{x}_0, \tilde{y}_0) = (0.309, 0.466)$, we can calculate the coefficients α_1, α_2 and we have

$$\alpha_1|_{(\tilde{x}_0,\tilde{y}_0)} \neq 0,\ \alpha_2|_{(\tilde{x}_0,\tilde{y}_0)} > 0,$$

so according to Theorem 3.1, system (1.5) undergoes a Flip bifurcation around $(\tilde{x}_0, \tilde{y}_0)$ and bifurcates to a two-periodic stable orbit. The result can be obtained by numerical simulation as Figure 1 and Figure 2.

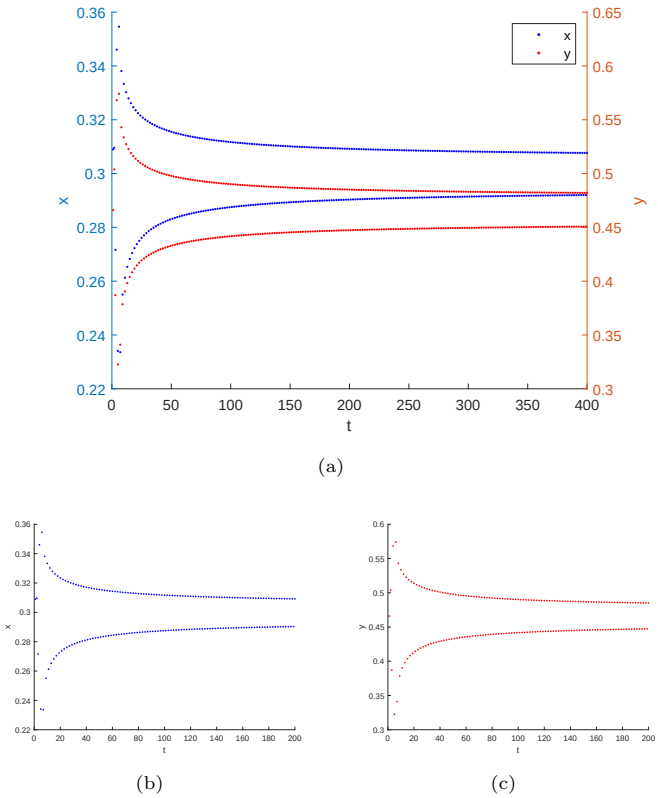

Figure 1. Flip bifurcation appears around the positive point $(\tilde{x}_0, \tilde{y}_0)$=(0.309, 0.466). The tendency of variables x and y with the transformation about time t is contrasted in (a). The period-two bifurcation scenarios for the variables x and y are shown in (b) and (c), respectively.

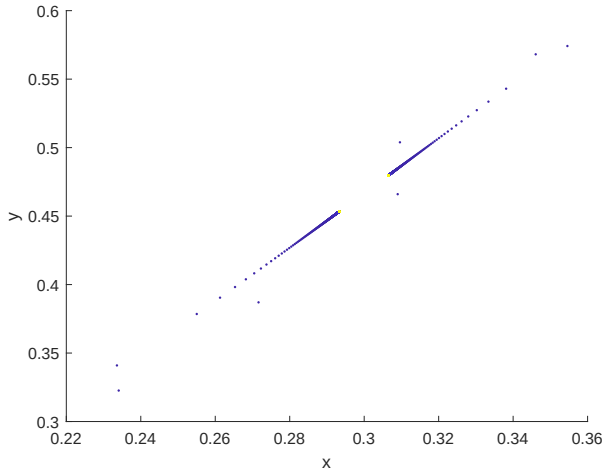

Figure 2. Phase diagrams at the positive point $(\tilde{x}_0, \tilde{y}_0)$=(0.309, 0.466). There exists a 2-periodic stable orbit around the point $(x_0, y_0) \approx (0.3, 0.46666667)$.

4.2. Numerical simulation of Hopf bifurcation

We still choose τ as the bifurcation parameter in curve N.S. The unique positive equilibrium point $(x_1, y_1) \approx (0.2280, 0.4780)$ of the model can be obtained by giving the parameters

$$\tau = 0.1509, r = 0.71, s = 0.15, m = 0.93, n = 0.71, z = 0.5, K = 4, K_2 = 0.5.$$

Then we can easily get the corresponding parameters in system (1.5):

$$a = 0.6549, c = 0.2113, k_1 = 0.1775, k_2 = 0.25.$$

By choosing the initial value of $(\tilde{x}_1, \tilde{y}_1) = (0.2285, 0.4785)$, we can calculate the coefficient $a^*|_{(\tilde{x}_1, \tilde{y}_1)}$ and we have

$$a^*|_{(\tilde{x}_1, \tilde{y}_1)} > 0,$$

so according to Theorem 3.2, model (1.5) undergoes a Hopf bifurcation around $(\tilde{x}_1, \tilde{y}_1)$ and bifurcates to an attracting closed invariant curve.
The result can be obtained by numerical simulation as Figure 3 and Figure 4.

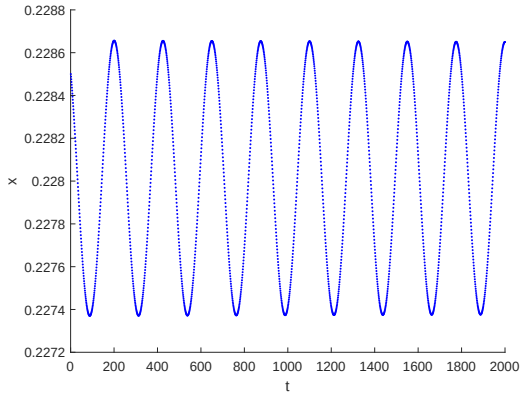

(a)

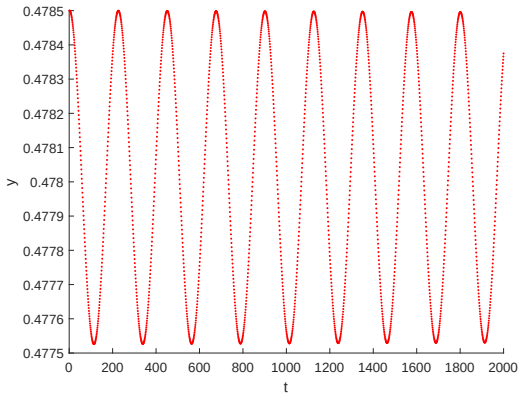

(b)

Figure 3. Hopf bifurcation appears around the positive point $(\tilde{x}_1, \tilde{y}_1) = (0.2285, 0.4785)$. (a) and (b) are the variations of x and y with the time t, respectively.

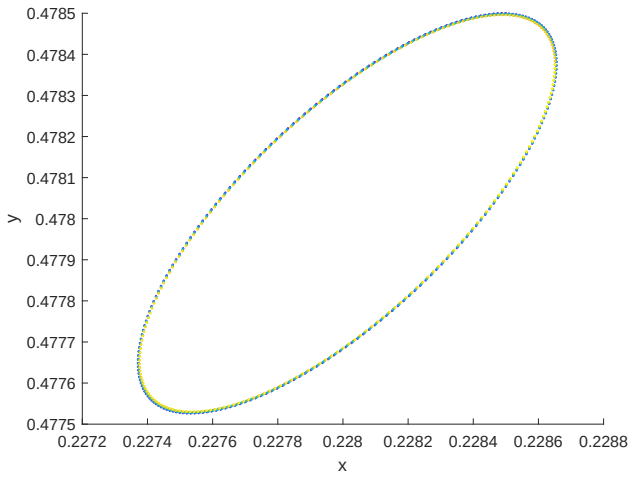

Figure 4. Phase diagrams at the positive point $(\tilde{x}_1, \tilde{y}_1) = (0.2285, 0.4785)$. There exists an attracting invariant closed curve around the point $(x_1, y_1) \approx (0.2280, 0.4780)$.

4.3. Chaos analysis

In this section, chaotic cases at bifurcating points are analyzed using numerical simulations. We give bifurcation diagrams, maximum Lyapunov exponents, and phase diagrams for a set of parameter to verify the chaotic cases.

According to chaos theory, we have the following Lemma 4.1 and Theorem 4.1.

Lemma 4.1. *[38] The expression of maximum Lyapunov index is given by:*

$$\lambda = \lim_{n\to\infty} \frac{1}{n} \sum_{n=0}^{n-1} ln \left| \frac{df(x_n, \mu)}{dx} \right|.$$

Theorem 4.1. *[38] If $\lambda < 0$, the neighboring points of the system are stable fixed points or generate periodic behavior. If $\lambda > 0$, the neighboring points are local instability and generate chaotic situations.*

4.3.1. Chaotic behavior near the Flip bifurcation point

In the following, we still select the set of parameters

$$\tau \approx 2.22222222222, r = 0.1, s = 0.18, m = 0.35, n = 0.8, z = 0.3, K = 2, K_2 = 0.1,$$

and we get

$$a = 1.05, c = 1.8, k_1 = 0.4, k_2 = 0.16666667.$$

After selecting the internal equilibrium point $(0.309, 0.466)$ and the perturbation $\delta \in (0, 0.06)$ with parameter k_1, we analyze the trend of x with δ by numerical simulation and obtain the chaotic bifurcating cases (see Figure 5). It can be seen that when the perturbation $\delta \in (0, 0.042)$, the value of the maximum Lyapunov exponent always oscillates around zero, so we cannot accurately describe the chaotic dynamic behavior of the parameter in this range. But when the perturbation $\delta \in (0.042, 0.054)$, we can notice that there exists period-7 solutions, this shows that

the system becomes to achieve a dynamical balance in this range and no chaotic situations occur. However, when the perturbation δ continues to increase, that is, $\delta \in (0.054, 0.056)$, then the chaotic behaviors will occur with the value of the maximum Lyapunov exponent is greater than zero. From an ecological perspective, chaotic behaviors mean that the system will fail to maintain a stable state or a periodic balance, leading to a state of disorder.

When we take a particular parameter $\delta = 0.0569$, that is, $k_1 = 0.4569$, the relevant phase diagram of the model (1.5) is displayed in Figure 6, which shows that the chaotic behaviors occur with the increase of the perturbation δ.

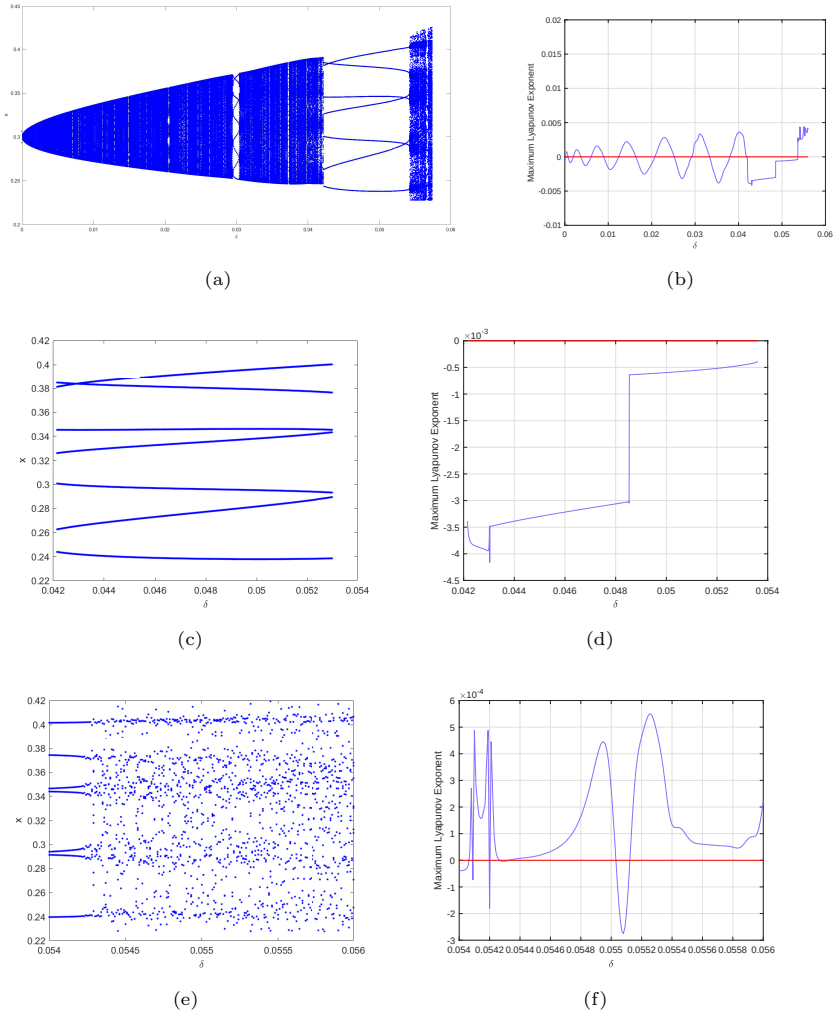

Figure 5. $\delta \in (0, 0.06)-$bifurcation diagram at the fixed point $(0.309, 0.466)$ contrasted with the maximum Lyapunov exponent. (a) and (b) show that the bifurcation diagram corresponds to the maximum Lyapunov exponent in the range of $\delta \in (0, 0.06)$. From figure (c) to figure (f), the two different dynamical behaviors will be shown by comparing the amplifications of the bifurcation diagrams and the maximum Lyapunov exponent in the same range of δ.

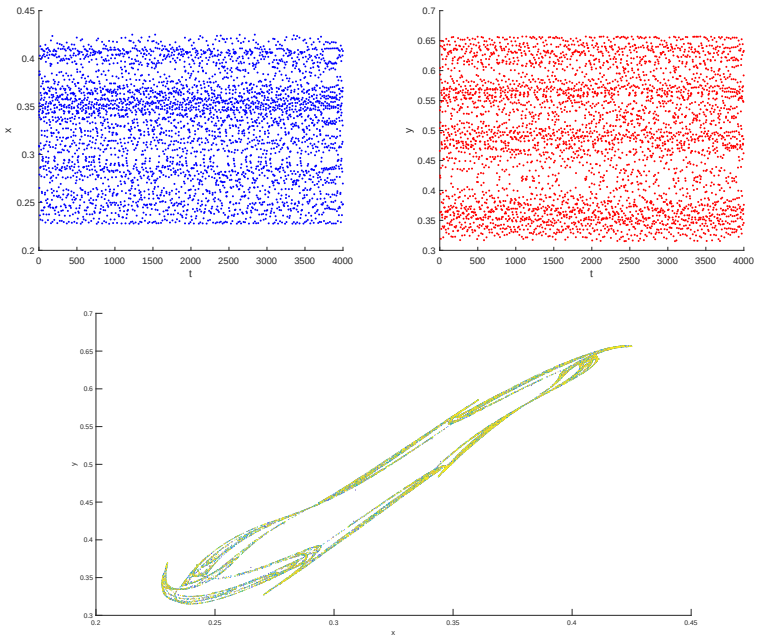

Figure 6. The phase diagram of the model (1.5) at the fixed point $(0.309, 0.466)$. This indicates that chaos occurs when the perturbation $\delta = 0.0569$.

4.3.2. Chaotic behavior near the Hopf bifurcation point

In this subsection, we still choose the set of parameters in section 4.2 to consider Hopf bifurcation with chaotic cases. That is

$$\tau = 0.1509, a = 0.6549, c = 0.2113, k_1 = 0.1775, k_2 = 0.25.$$

After choosing perturbation parameter $\delta \in (-0.2, 2.1)$ with step length τ, we can obtain bifurcation diagram and the corresponding maximum Lyapunov exponent(See Figure 7). When the maximum Lyapunov exponent goes from negative to positive, the stability of the system is gradually destroyed and eventually enters a chaotic state within this set of parameters.

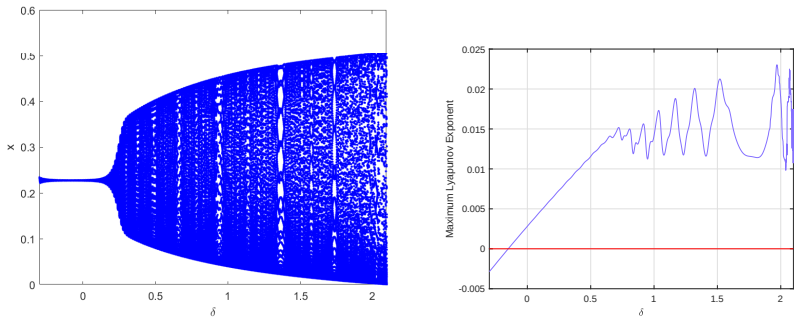

Figure 7. The bifurcation diagram and maximum Lyapunov exponent corresponding to perturbation $\delta \in (-0.2, 2.1)$ for x.

5. Conclusions

In this paper, we study local dynamical behaviors of the modified Holling-Tanner system with discrete time. We prove that the system (1.5) has a trivial equilibrium and two boundary equilibria. We pay more attention to the unique positive equilibrium point $E_*(x^*, y^*) = (\frac{1-a-k_1+\sqrt{(1-a-k_1)^2-4(ak_2-k_1)}}{2}, \frac{1-a-k_1+\sqrt{(1-a-k_1)^2-4(ak_2-k_1)}}{2} + k_2)$. We prove that if Flip bifurcation and Hopf bifurcation occurs at $E_*(x^*, y^*)$, the bifurcation curve U_1 and N.S must be satisfied respectively. Then the corresponding results of bifurcation behavior are obtained. Next, we provide numerical simulations to verify our theoretical discussions. We can see there exists a 2−periodic stable orbit from the positive point when we choose a set of parameters. Similarly, an attracting closed invariant curve bifurcates from the positive equilibrium in Hopf circumstances. By numerical simulations, it can be found that both Flip bifurcation and Hopf bifurcation will produce chaos.

Biologically, the predator in system (1.5) is called generalist, which have several alternative food sources by increasing an additional carrying ability K_2. According to the discussion in Lemma 2.2, the positive equilibrium $E_*(x^*, y^*)$ must meet the condition $k_2 < \frac{k_1}{a}$, which is equivalent to $K_2 < \frac{nr}{m}$ in system (1.2), and n, r, m are constants. Therefore, the condition we propose is of practical significance. Furthermore, the occurrence of Flip bifurcation indicates that the densities of predators and prey will be stable around a 2−period state eventually. And the appearance of Hopf bifurcation implies that predators and prey will coexist with periodic oscillations. By regulating the range of bifurcation parameters, we can acquire the desired densities of the system and avoid the occurrence of chaotic cases.

In future work, the system can be studied using different discrete methods, such as the improved Euler method. In addition, new bifurcation parameters will be chosen. We also hope to do further discussions on codimension two bifurcations, such as strong resonances.

References

[1] Sez E, Gonzlez-Olivares E. Dynamics of a predator-prey model. SIAM Journal on Applied Mathematics, 1999, 59(5): 1867-1878.

[2] Georgescu P, Hsieh Y H. Global dynamics of a predator-prey model with stage structure for the predator. SIAM Journal on Applied Mathematics, 2007, 67(5): 1379-1395.

[3] Mortoja S G, Panja P, Mondal S K. Dynamics of a predator-prey model with stage-structure on both species and anti-predator behavior. Informatics in medicine unlocked, 2018, 10: 50-57.

[4] Ghanbari B, Djilali S. Mathematical analysis of a fractional-order predator-prey model with prey social behavior and infection developed in predator population. Chaos, Solitons & Fractals, 2020, 138: 109960.

[5] Xiang C, Huang J, Wang H. Linking bifurcation analysis of HollingTanner model with generalist predator to a changing environment. Studies in Applied Mathematics, 2022, 149(1): 124-163.

[6] Aziz-Alaoui M A. Study of a Leslie-Gower-type tritrophic population model. Chaos, Solitons & Fractals, 2002, 14(8): 1275-1293.

[7] Cushing J M. Nonlinear semelparous Leslie models. Mathematical Biosciences & Engineering, 2005, 3(1): 17-36.

[8] Zhu Z, Chen Y, Li Z, et al. Stability and bifurcation in a LeslieGower predator-prey model with Allee effect. International Journal of Bifurcation and Chaos, 2022, 32(03): 2250040.

[9] Freedman H I, Mathsen R M. Persistence in predator-prey systems with ratio-dependent predator influence. Bulletin of Mathematical Biology, 1993, 55(4): 817-827.

[10] Jia X, Huang K, Li C. Bifurcation Analysis of a Modified LeslieGower PredatorPrey System. International Journal of Bifurcation and Chaos, 2023, 33(02): 2350024.

[11] Hsu S B, Huang T W. Global stability for a class of predator-prey systems. SIAM Journal on Applied Mathematics, 1995, 55(3): 763-783.

[12] Oaten A, Murdoch W W. Functional response and stability in predator-prey systems. The American Naturalist, 1975, 109(967): 289-298.

[13] Chiou J M, Mller H G, Wang J L. Functional response models. Statistica Sinica, 2004: 675-693.

[14] Yu S. Global stability of a modified Leslie-Gower model with Beddington-DeAngelis functional response. Advances in Difference Equations, 2014, 2014(1): 1-14.

[15] Chen H, Zhang C. Dynamic analysis of a LeslieGower-type predatorprey system with the fear effect and ratio-dependent Holling III functional response. Nonlinear Analysis: Modelling and Control, 2022, 27(5): 904-926.

[16] Holling C S. The functional response of invertebrate predators to prey density. The Memoirs of the Entomological Society of Canada, 1966, 98(S48): 5-86.

[17] Skalski G T, Gilliam J F. Functional responses with predator interference: viable alternatives to the Holling type II model. Ecology, 2001, 82(11): 3083-3092.

[18] Dawes J H P, Souza M O. A derivation of Holling's type I, II and III functional responses in predatorprey systems. Journal of theoretical biology, 2013, 327: 11-22.

[19] Arsie A, Kottegoda C, Shan C. A predator-prey system with generalized Holling type IV functional response and Allee effects in prey. Journal of Differential Equations, 2022, 309: 704-740.

[20] Tripathi J P, Bugalia S, Tiwari V, et al. A predatorprey model with Crowley-Martin functional response: A nonautonomous study. Natural Resource Modeling, 2020, 33(4): e12287.

[21] Li X, Liu Y. Transcritical bifurcation and flip bifurcation of a new discrete ratio-dependent predator-prey system. Qualitative Theory of Dynamical Systems, 2022, 21(4): 122.

[22] Arancibia-Ibarra C, Flores J D, Pettet G, et al. A HollingTanner predatorprey model with strong Allee effect. International Journal of Bifurcation and Chaos, 2019, 29(11): 1930032.

[23] Roy B, Roy S K. HollingTanner model with BeddingtonDeAngelis functional response and time delay introducing harvesting. Mathematics and Computers in Simulation, 2017, 142: 1-14.

[24] Mandal P S, Banerjee M. Stochastic persistence and stability analysis of a modified HollingTanner model. Mathematical Methods in the Applied Sciences, 2013, 36(10): 1263-1280.

[25] Aziz-Alaoui M A, Okiye M D. Boundedness and global stability for a predator-prey model with modified Leslie-Gower and Holling-type II schemes. Applied Mathematics Letters, 2003, 16(7): 1069-1075.

[26] Okiye M D, Aziz-Alaoui M A. On the dynamics of a predator-prey model with the Holling-Tanner functional response. Mathematical modelling & computing in biology and medicine, 2002, 1: 270-278.

[27] Yu S. Global asymptotic stability of a predator-prey model with modified Leslie-Gower and Holling-type II schemes. Discrete Dynamics in Nature and Society, 2012.

[28] Zhang X, Zhang C, Zhang Y. Pattern dynamics analysis of a time-space discrete FitzHugh-Nagumo (FHN) model based on coupled map lattices. Computers & Mathematics with Applications, 2024, 157: 92-123.

[29] Hong B, Zhang C. Bifurcations and chaotic behavior of a predator-prey model with discrete time. AIMS Mathematics, 2023, 8(6): 13390-13410.

[30] Li T, Zhang X, Zhang C. Pattern dynamics analysis of a spacetime discrete spruce budworm model. Chaos, Solitons & Fractals, 2024, 179: 114423.

[31] Mid E C, Dua V. Parameter estimation using multiparametric programming for implicit Eulers method based discretization. Chemical Engineering Research and Design, 2019, 142: 62-77.

[32] Liu X, Xiao D. Complex dynamic behaviors of a discrete-time predatorprey system. Chaos, Solitons & Fractals, 2007, 32(1): 80-94.

[33] Wang C, Li X. Stability and Neimark-Sacker bifurcation of a semi-discrete population model. J. Appl. Anal. Comput, 2014, 4(4): 419-435.

[34] Wiggins S. Introduction to Applied Nonlinear Dynamic Systems and Chaos 2d. 2000.

[35] Ma R, Bai Y, Wang F. Dynamical behavior analysis of a two-dimensional discrete predator-prey model with prey refuge and fear factor. Journal of Applied Analysis and Computation, 2020, 10(4): 1683-1697.

[36] Yang Y, Abdullah T Q S, Huang G, et al. Mathematical Analysis of SIR Epidemic Model with Piecewise Infection Rate and Control Strategies. Journal of Nonlinear Modeling and Analysis, 2023, 5(3): 524-539.

[37] Kuznetsov Y A, Kuznetsov I A, Kuznetsov Y. Elements of applied bifurcation theory. New York: Springer, 1998.

[38] Pecora L M, Carroll T L. Synchronization in chaotic systems. Physical review letters, 1990, 64(8): 821-824.